Transmit-array antenna design for broadband backhaul 5G communications at WiGiG band

Sérgio A. Matos[1,2], Jorge R. Costa[1,2], Carlos A. Fernandes[1,3], Nour Nachabe[4], Cyril Luxey[4], Diane Titz[4], Frederic Gianesello[7], Carlos Del-Río[6], Ana Arboleya[5], Jorge P. Teixeira[1,2], Jean-Philippe Garnero[4], Jean-François Vizzari[4].

[1] Instituto de Telecomunicações, Lisbon, Portugal, sergio.matos@lx.it.pt

[2] Department of Information Science and Technology, University Institute of Lisbon, Lisbon, Portugal

[3] Instituto Superior Técnico, IT/IST, Lisbon, Portugal

[4] Polytech'Lab, Université Nice Sophia Antipolis, 06560 Valbonne, France.

[5] Universidad Rey Juan Carlos, Madrid, Spain.

[6] Universidad Pública de Navarra, UPNA, Pamplona, Spain.

[7] STMicroelectronics, 38920 Crolles, France.

***Abstract*—A cost-effective transmit-array (TA) antenna design framework is presented and experimentally validated for 5G backhaul applications at the WiGiG band. The antenna is composed of a discrete dielectric lens (DDL) fed by a horn, specifically designed for this application. Both the TA and feed are fabricated using additive manufacturing. Metal coating and Fuse Deposition Modeling (FDM) are employed for the horn and TA fabrication, respectively. Simple design rules are devised to quantify the bandwidth of this type of antennas as function of the aperture dimension D and focal distance F. Based on this framework a compact TA antenna ($F/D = 0.5$) than can comply with typical specifications for 5G backhaul links at WiGiG band (minimum gain of 30 dBi from 57 to 66 GHz) is designed.**

***Index Terms*—5G mobile communication, backhaul communications, WiGiG band, Transmit-Array, V-band Horn antenna, 3D-Printing, Metal coating .**

I. INTRODUCTION

The massification of 5G will pivot on cost-effective technologies that can support the exponential growth of data demand fomented by the era of Internet of Things (IoT). The landscape of future 5G mobile communications will include pico and femto cells,. Therefore, extremely low-cost backhaul links between base stations and access points are required. Millimeter-waves (mmW) provide the necessary throughputs with extremely low-cost deployment capability when compared with fibre optics-based backhaul solutions. In particular, the WiGiG band from 57 to 66 GHz, offers large bandwidths over unlicensed spectrum and high frequency reused capability, ideal in dense cell's environments [1]. The main challenge is to conciliate high gain with low cost, both bounded by the necessary fabrication precision at millimeter frequencies. Phased-array configurations could be an option, but they lead to excessive feeding network losses and their cost scale with gain and frequency [2] as well as DC consumption. An intensive research effort is being made on presenting the most low-cost solution that can deliver high gain (typically above 30 dBi) in the entire WiGiG band [3]-[5]. Dielectric lens-based solutions benefit from the recent developments of fused deposition modeling (FDM), which is the most affordable 3D printing technology. The drawback is that 3D FDM materials tend to be lossy, such as ABS-M30 ($\varepsilon_r = 2.48$ $\tan\delta \approx 0.009$) and PLA ($\varepsilon_r = 2.9$ $\tan\delta \approx 0.015$). In [6], the authors showed that this problem could be circumvented by using a transmit-array (TA) lens – sometimes designated as discrete dielectric lens (DDL). We showed that the antenna radiation efficiency increased from 60% to 83% when a PLA chopped elliptical lens is replaced by an equivalent PLA TA. Achieving high gain is quite straightforward, however, the challenge is to overcome the bandwidth limitation caused by number of 360º phase correction zones, that directly correlates with the F/D ratio. In this work, we quantify the relation between F/D ratio and the bandwidth of TA. As far as the authors are aware, it is still lacking this type of design guidelines that clearly defines the limits of applicability of DDL for broadband applications. A DDL using ABS-M30 ($\varepsilon_r = 2.48$, $\tan\delta \approx 0.009$) is then devised according to the specifications of 5G backhaul connections at WiGiG band. A compact corrugated horn antenna with high radiation efficiency (>85%) and low cross polarization (>27 dB) in the entire WiGiG band is designed to feed the TA. A very good agreement between measurements and simulations validate the developed design rules and also show that TA antennas can be a viable alternative as low-cost antennas for future 5G backhaul links.

In section II, the design guidelines for a DDL are provided based on a GO/PO analysis. In section III, we implement these guidelines to design an antenna (feed and lens) compliant with the gain specifications for WiGiG 5G backhaul links. Finally, in section IV measurement results are presented.

I. Dielectric Transmit-Array

The aperture is designed to produce boresight collimation by distributing the unit cells that compose the TA to create a plane of constant phase perpendicular to the lens aperture. The resulting TA can then be built as a single dielectric block, thus compatible with FDM 3D printing. Each unit cell is a parallelepiped with height h_{max}, composed of a dielectric (ABS-M30) with height h and air (occupying the remaining volume). The control of the unit cell phase shift is obtained by varying the dielectric height h, that can be approximated by $\phi_{lens}(h) \approx -(\sqrt{\varepsilon_r}-1)k_0 h - k_0 h_{max}$, where ε_r is the real part of the dielectric permittivity and k_0 is the free-space wavenumber. Thus imposing $\Delta\phi_{out} = 2m\pi$ the profile of the lens is obtained

$$h(r) = h_0 + \frac{F - \Delta l \ + m\lambda_0}{\sqrt{\varepsilon_r}-1}, R_m < r < R_{m+1} \tag{1}$$

Where h_0 is the central height of the lens ($r = 0$), $\Delta l = \sqrt{r_i^2 + F^2} - F$ (see Fig. 1) and m defines the zone of the lens up to a total of K zones. The radial positions of the transitions between zones are defined by the condition $h(R_m) = h_{min}$. We considered the typical half wavelength unit cell size, $w = 2.5\ mm\ \left(\frac{\lambda_0}{2} @\ 60\ GHz\right)$ resulting in the stepwise lens profile given in Fig. 1. The radial symmetry of this problem allows assembling the lens using concentric annuli with fixed widths w, as represented in the inset of Fig. 1. The diffraction effects are then reduced when compared with a full pixelized version of the lens.

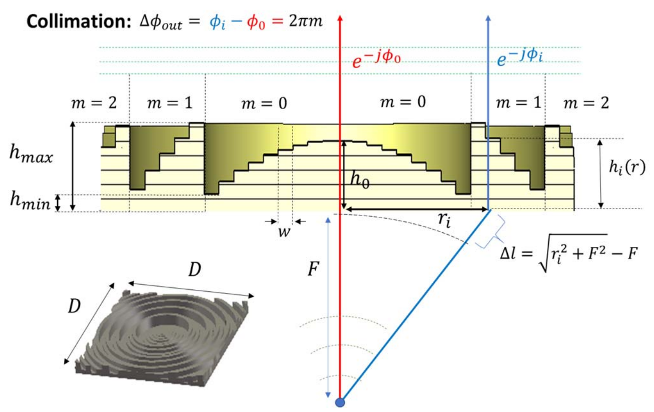

Fig. 1. Working principle of a dielectric transmit-array for beam collimation.

The outgoing electric field from the TA in a plane of constant phase (green dashed lines in Fig. 1) can be model by gaussian amplitude distribution with standard deviation σ by

$$\vec{E}_{ab}(r) = e^{-\frac{r^2}{2\sigma^2}} e^{j\Phi_{out}} \vec{u}_E. \tag{2}$$

where Φ_{out} varies with wavelength as a stepwise function

$$\Phi_{out} = -2\pi m \frac{\lambda_0}{\lambda},\ R_m < r < R_{m+1}. \tag{3}$$

With $m = \{0,1,..,K\}$. The standard deviation σ is directly related to the taper level, τ_{dB}, $E_{ab}(r = D/2) = 10^{-\tau_{dB}/20}$

$$\sigma = \frac{D}{2}\sqrt{\frac{10\log_{10} e}{\tau_{dB}}} \tag{4}$$

As the position of the 360º phase transitions depends on the operating frequency, phase errors build-up as the number of lens zones increases. By integrating the fields of the aperture using GO/PO analysis the directivity for the boresight direction can be calculated explicitly

$$D_{max} = D_{ir0}\left|\frac{\sum_{m=0}^{K} e^{-j\frac{2\pi m\lambda_0}{\lambda}}\left(e^{-\frac{R_m^2}{2\sigma^2}} - e^{-\frac{R_{m+1}^2}{2\sigma^2}}\right)}{1 - e^{-\frac{D^2}{4\sigma^2}}}\right|^2. \tag{5}$$

Where

$$D_{ir0} = s_{TA}\left(\frac{4\pi\sigma}{\lambda}\right)^2 \tanh\left[\left(\frac{D}{4\sigma}\right)^2\right] \tag{6}$$

is the directivity of an aperture with constant phase ($\lambda = \lambda_0$) and Gaussian illumination, as in Eq.8 of [7]. R_m is defined by $h_i(R_m) = h_{min}$ with $m = \{0,1,..,K\}$ and since the last zone can be truncated, $R_{K+1} = D/2$. We introduce the parameter s_{TA} as the TA scaling factor that accounts for other effects that were not considered in this GO/PO analysis, such as unit cell reflection and insertion losses, aperture illumination spillover and phase errors caused by refraction and diffraction (which are more significant near the lens 360º phase transitions). Looking at a wide variety of different types of TAs, s_{TA} is typically below 50% [7]. Therefore, we considered $s_{TA} = 50\%$ for the design process. As shown in [6], the aperture efficiency of these dielectric TAs is high, allowing to approximate the antenna gain by its directivity. The aperture dimension and the focal distance can then be defined from a given gain and bandwidth criteria according to (5) and (6).

II. Transmit-Array Antenna for WiGiG Band

An antenna for 5G backhaul wireless links needs to deliver high gain, typically above 30 dBi [1]. WiGiG band usually refers to the [57-66] GHz band according to 802.11.ad standard, but recently an extended WiGiG band was defined (802.11.ay) covering [57-70] GHz.

A. TA design

We set a 32 dBi directivity D_0, to give a 2 dB margin to accommodate in the specified gain criteria the bandwidth limitation of the TA. The aperture dimension follows from (6): $D_0(D) = 32\ (\text{dBi}) \to D \approx 100\ (\text{mm})$. The maximum number of phase transitions is determined by the F/D ratio, where F is the focal distance. For this aperture size, we use equation (5) to estimate the minimum focal distance that complies with the 30-dBi minimum gain criteria of the WiGiG band. By setting $h_0 = h_{max}$ the radius of the first lens zone ($m = 0$), which has no bandwidth limitation, is maximum. Neglecting second order effects, this condition maximizes the lens bandwidth as well. Later, full-wave simulations are employed to tune this parameter, further optimizing the gain and lens bandwidth. In Fig. 2 we plot (5) for several F/D ratios and select the minimum value that complies with the gain criteria for the WiGiG band, corresponding to $F/D = 0.5$. Fig. 2 captures the interplay between the dependence of D_{max} with frequency and the gain degradation due to the phase error caused by zoning process. For $F/D > 2$ no zoning occurs ($K = 0$) thus $D_{max} = D_0$.

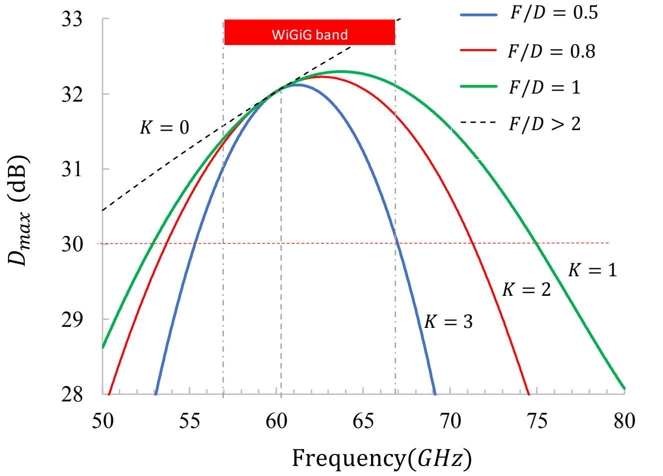

Fig. 2. GO/PO directivity D_{max} variation with frequency, Eq. (5), for different focal distances considering an aperture size of $D = 100\ mm$ and taper of 15 dBi and $s_{TA} = 50\%$.

As mentioned, after defining the dimensions of the TA it is possible to further tune h_0. We performed several full wave simulations of the lens illuminated by a Gaussian beam with different h_0 values looking for the maximum gain at 60 GHz and, at the same time, the minimum gain variation between 57 GHz and 66 GHz. This optimization led to $h_0 = h_0^{opt} = 6.67\ mm$.

B. Feed design

A corrugated horn antenna was designed to be compact ($8 \times 5 \times 22\ mm$), wideband and have a stable radiation pattern in the WiGiG band (57-66 GHz). The fabrication was done by metal coating a 3D-printed dielectric cast. The performance of this design is shown in Fig. 3. A 13 dBi co-pol gain was achieved from 56 to 67 GHz as well as good polarization purity (>27 dBi from 50-67 GHz). Measured and simulated gains agree very well.

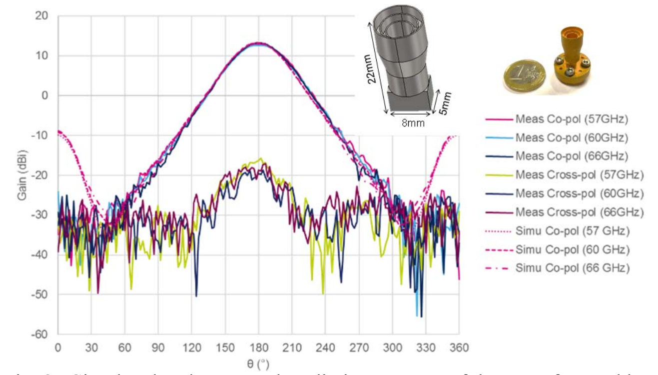

Fig. 3. Simulated and measured Radiation patterns of the manufactured horn antenna in the WiGiG band.

III. MEASUREMENTS

The measurement campaign of the full antenna-system was conducted in our in-house measurement system: a spherical measurement range capable of performing amplitude-only acquisitions up to 140 GHz at fixed distances of 20 cm, 40 cm and 60 cm. Considering the main diagonal of the lens ($D_{diag} = \sqrt{2}D$), the far-field (FF) distance at 66 GHz is 8.8 m, thus, it was necessary to resort to near-field to far-field (NF-FF) transformation techniques. The employed phaseless NF-FF algorithm is based on the method presented in [7]. It is an iterative phaseless technique which relies on the spatial variability of the NF with distance and, therefore, it requires amplitude information from two or more NF acquisition surfaces. The main advantage of iterative techniques is that they do not require any modification of the measurement setup with respect to a regular FF acquisition, however there is a risk of stagnation of the algorithm due to the use of iterative solvers for nonlinear systems of equations. This risk becomes higher when variability of the field within the NF acquisition surfaces is low, as might be the case with lens antennas, yielding less accurate FF results. The field was acquired at two spherical surfaces with radii of 40 cm and 60 cm respectively. The sampling rate was /4 at the highest frequency of the band, 66 GHz, as required to perform phaseless NF-FF transformations. Due to mechanical restrictions in the setup, the acquisition surfaces were truncated to a • and angular range of [-25º, 25º], yielding a valid margin of the FF data of [-14º, 14º] in both axes. In Fig. 4 the FF amplitude and phase of the copolar component of the field, computed from the NF phaseless acquisitions are compared with full-wave simulations for the E-plane of the copolar component. The agreement between measurements and simulations is good within the valid margin area, differences may arise from the error accumulated though all the postprocessing steps to obtain the FF radiation pattern from NF phaseless data. Finally, the antenna gain was computed by means of the well-known intercomparison method [9] with a standard gain horn. Since the lens antenna gain was measured in the NF region, the variation introduced by the NF-FF transformation should be compensated as follows:

$$G_{lens,FF} = G_{lens,NF} + \left(D_{lens,FF} - D_{lens,NF}\right) \quad (7)$$

where $G_{lens,NF}$ is the measured gain in NF, 27.16 dBi at 60 GHz. $D_{lens,FF}$ and $D_{lens,NF}$ are directivities from FF and NF respectively, computed from pattern integration. The final FF gain values for the rest of the studied frequencies are gathered in TABLE 1 and compared with the results obtained from simulations and GO/PO analysis. Gain is higher than the required 30 dBi within the complete operating band.

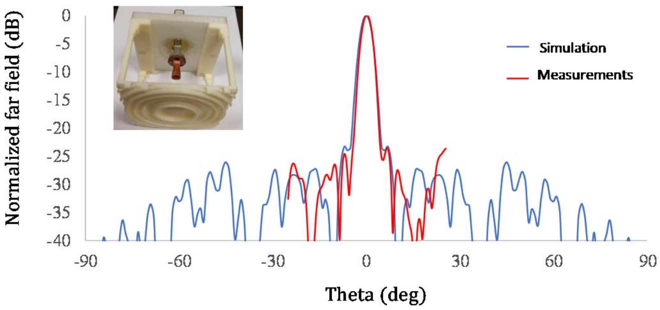

Fig. 4. Measured and simulated normalized radiation pattern (E-plane) at 60 GHz for the co-pol component of the far-field. The valid margin of the NF-FF transformation is shaded in grey.

TABLE 1.
FAR-FIELD GAIN COMPARISON FOR THE STUDIED FREQUENCIES.

FF Gain (dBi)	GO/PO	Full wave	Measurements + NF-FF
$f = 57\,GHz$	31.0	30.5	32.2
$f = 60\,GHz$	32.0	31.8	32.2
$f = 63\,GHz$	31.9	31.9	31.3
$f = 66\,GHz$	30.7	29.9	29.8

IV. CONCLUSIONS

A low-cost 3D printed antenna for 5G backhaul communications at WiGiG was designed and fabricated. Experimental results validated our design rules that, although based on GO/PO analysis, show to be quite effective for frequency bandwidth control in this type of transmit-arrays antennas. In known designs, the *F/D* ratio is defined using heuristic assumptions. Herein, a closed form expression was presented to find the optimal *F/D* ratio of the antenna according to gain and bandwidth criteria. A horn antenna for the V-band was also designed for this specific application. This design privileged a simple fabrication process based on the most affordable 3D printing techniques, making it a cost-effective alternative to existing solutions for mm-wave high-gain antennas.

ACKNOWLEDGMENT

This work was partially supported by grant ISTA-BM-2016 and partially supported by Fundação para a Ciência e Tecnologia (FCT) under projects PTDC/EEI-TEL/30323/2017 (“ADAM3D”) and UID/EEA/50008/2019.

REFERENCES

[1] ECC Report 288: “Conditions for the coexistence between Fixed Service and other envisaged outdoor uses/applications in the 57-66 GHz range”, Jan. 2019.

[2] U. Rüddenklau, “mmWave Semiconductor Industry Technologies: Status and Evolution,” ETSI white paper Nº 15 second edition (2018).

[3] L. Dussopt *et al.*, "A V-Band Switched-Beam Linearly Polarized Transmit-Array Antenna for Wireless Backhaul Applications," in *IEEE Transactions on Antennas and Propagation*, vol. 65, no. 12, pp. 6788-6793, Dec. 2017.

[4] N. Nachabe, C. Luxey, D. Titz, J. R. Costa, S. A. Matos, F. Gianesello, C. A. Fernandes, "Low-cost 60 GHz 3D printed lens fed by a planar source with WR15 transition integrated on FR4 PCB," 2017 IEEE International Symposium on Antennas and Propagation & USNC/URSI National Radio Science Meeting, San Diego, CA, 2017, pp. 2671-2672.

[5] C. Jouanlanne, A. Clemente, M. Huchard, J. Keignart, C. Barbier, T. Le Nadan, L. Petit, "Wideband Linearly Polarized Transmitarray Antenna for 60 GHz Backhauling," in IEEE Transactions on Antennas and Propagation, vol. 65, no. 3, pp. 1440-1445, March 2017.

[6] J. P. Teixeira, S. A. Matos, J. R. Costa, C. A. Fernandes, N. Nachabe, C. Luxey, D. Titz, , F. Gianesello, "Transmit array as a viable 3D printing option for backhaul applications at V-band," 2017 IEEE International Symposium on Antennas and Propagation & USNC/URSI National Radio Science Meeting, San Diego, CA, 2017, pp. 2641-2642.

[7] E. B. Lima, S. A. Matos, J. R. Costa, C. A. Fernandes and N. J. G. Fonseca, "Circular Polarization Wide-Angle Beam Steering at Ka-Band by In-Plane Translation of a Plate Lens Antenna," in IEEE Transactions on Antennas and Propagation, vol. 63, no. 12, pp. 5443-5455, Dec. 2015.

[8] Y. Álvarez, F. Las-Heras, M. R. Pino, “The sources reconstruction method for amplitude-only field measurements,” IEEE Transactions on Antennas and Propagation, vol. 58, no. 8, pp. 2776-2781, August 2010.

[9] IEEE Standard test procedures for antennas, ANSI/IEEE Std 149-1979.